Synthesis and thermal analysis of linear triblock copolymers based on methacrylate ester

Bo Lin · Hongdong Zhang · Yuliang Yang

Abstract Two linear triblock copolymers poly(*t*-butyl methacrylate-*b*-2-hydroxyl ethyl methacrylate-*b*-*N*,*N*-dimethylaminoethyl methacrylate) (P*t*BMA$_{97}$-*b*-PHEMA$_{18}$-*b*-PDMAEMA$_{98}$) and poly(*t*-butyl methacrylate-*b*-glycidyl methacrylate-*b*-styrene) (P*t*BMA$_{137}$-*b*-PGMA$_{23}$-*b*-PSt$_{156}$) were controlled synthesized with living RAFT polymerization technique under the chain transfer of cumyl dithiobenzoate. The results of FT-IR spectra illustrate that the characteristic groups of copolymer fit well with the result of ^{1}H-NMR, which successfully determines the corresponding molecular structure of triblock copolymers. The thermal stability of P*t*BMA-*b*-PGMA-*b*-PSt and P*t*BMA-*b*-PHEMA-*b*-PDMA-EMA was also complementarily explained by the activation energy of thermal decomposition from Friedman differential method and Ozawa–Flynn–Wall integral method. The results show that the degradation energy of the former copolymer was much higher than that of the latter copolymer, because the aromatic groups were introduced into the polymer segments of the former copolymer during the RAFT polymerization process, and the other reason is the oxirane rings are typically reactive which they occurred intermolecular crosslinking reaction during the thermal decomposition.

Keywords Methacrylate ester · Linear triblock copolymer · Thermogravimetry · Friedman analysis · Ozawa–Flynn–Wall analysis

B. Lin · H. Zhang (✉) · Y. Yang
Key Laboratory of Molecular Engineering of Polymer, Ministry of Education, and Department of Macromolecular Science, Fudan University, Shanghai 200433, China
e-mail: zhanghongdong@gmail.com

B. Lin
e-mail: jidalinbo@yahoo.com.cn

Introduction

It is a challenge to avoid agglomeration by itself in synthesis and processing of nanoscale materials due to its high specific surface area, tendency to form irreversible agglomerates or even restack through van der Waals effect interactions between the surfaces of the materials [1]. The surface functionalization of different dimensional material, such as zero-dimensional material (silica sphere), one-dimensional material of rare earth hydroxides (Y(OH)$_3$), and two-dimensional material of layered double hydroxide (LDH), is not only to prevent agglomeration of materials in a solvent or matrix but is an efficient way to assemble the materials at liquid–liquid interfaces to fabricate two-dimensional structures or to form encapsulations of water-in-oil (w/o) and oil-in-water (o/w) solutions [2–7]. Using asymmetric Y-shaped triblock copolymers planted on the surface of the spherical particles or the plane material of montmorillonite manocomposites to prepare hairy nanoscale materials as polymer chain brushes can well improve the wettability of nanomaterial [8]. These artificial amphiphilic nanoparticles and nanoplatelets not only disperse easily in many solvents with different polarities but fabricate ultrathin capsules and films that exhibited advantaged mechanical strength [9, 10].

Based on these, linear triblock copolymers were not only successfully synthesized, but also had been functionalized onto the surface of nanodiamond particles [2, 8]. This study aims to study the thermal property of the copolymer synthesized based on methacrylate ester. Therefore, we outline a process for preparing an amphiphilic linear triblock copolymer P*t*BMA-*b*-PHEMA-*b*-PDMAEMA where in the middle segment of PHEMA with active functional group of hydroxyl (containing the hydroxyl group) and in the other two polymer segments,

one arm (PDMAEMA) is hydrophilic and the other arm (P*t*BMA) is hydrophobic. Another potential amphiphilic triblock copolymer P*t*BMA-*b*-PGMA-*b*-PSt was synthesized by the RAFT polymerization technique as well because the segment of P*t*BMA hydrolyzed with trifluoroacetic acid was changed into an amphiphilic one P*t*MAA.

The thermal degradation of polymers has been studied quite extensively using thermogravimetry [11–16]. Herein, two isoconversional thermokinetic methods, Friedman differential method and Ozawa–Flynn–Wall (OFW) integral method, were applied on the triblock copolymers to explain the thermal degradation progress of polymer segments and the thermal stability in the thermal decomposition process.

Experimental

Materials

N,N-Dimethylaminoethyl methacrylate (DMAEMA, Aldrich, 98 wt%), styrene (St, Shanghai Chemicals Co. Ltd., 99 wt%), glycidyl methacrylate (GMA, ACROS, 99.9 wt%), 2-hydroxyl ethyl methacrylate (HEMA, Aldrich, 98 wt%), and *t*-butyl methacrylate (*t*BMA, TCI, 96 wt%) were distilled before use. 2,2′-Azobis(isobutyronitrile) (AIBN, 99 wt%) was purchased from Shanghai 4th Factory of Chemicals and was recrystallized from methanol. All solvents of benzene, methanol, tetrahydrofuran (THF, 99.5 wt%), chloroform ($CHCl_3$, 99.5 wt%), and *N,N′*-dimethylformamide (DMF, 99.0 wt%) were purchased from Aldrich Feida Chemicals, Shang district company and were dried over CaH_2 and distilled over Na/benzophenone. Cumyl dithiobenzoate (CDB, 99.0 wt%, $M_n = 272$ g mol^{-1}) was prepared according to the literature [17]. Deuterated chloroform (D, 99.9 wt%) used for ^{1}H-NMR test was supplied by Cambridge Isotope Laboratories, Inc., Andover, MA, USA.

Instruments and measurements

Gel permeation chromatography (GPC) was performed on a Waters 410 system equipped with three TSK-GEL H-type columns (particle size: 5.0 μm, M_w range: 0–10^3 g mol^{-1}, 0–2×10^4 g mol^{-1}, and particle size: 6.0 μm, M_w range: 0–4×10^5 g mol^{-1}), a Waters 410 RI detector, and a Waters 486 UV detector (254 nm), using THF as the eluent at a flow rate of 1 mL min^{-1} at 40 °C. The columns were calibrated by narrow polystyrene (M_w range: 200–3×10^6 g mol^{-1}) standards.

Fourier transform infrared spectroscope spectra were obtained on a NEXUS-470 FTIR instrument (Thermo Nicolet, U.S.A.). To minimize uneven light scattering, samples which are dispersed in KBr pellets should be ground to as small a particle size as possible, before the pellet is pressed.

^{1}H-NMR measurements were carried out on a Bruker (500 MHz) NMR instrument (Bruker, Switzerland), using deuterated chloroform as solvent and tetramethylsilane (TMS) as reference.

The thermostability of samples was analyzed by thermogravimetry analysis (TG, TGA Q5000 (QNX, TA), USA) and derivative thermogravimetry analysis (DTG) with a balance purge flow rate of 10 mL min^{-1} and a sample purge flow rate of 25 mL min^{-1} in a dynamic N_2 atmosphere. About 4–6 mg of sample was placed in a platinum cell that was transferred to the detector plate, and the furnace was then heated at the given four heating rates (5, 10, 20, and 40 °C min^{-1}).

Every 5 °C was adopted from the raw data of the TG at each appointed heating rate and carried out for kinetic analysis in the temperature range between 100 and 550 °C. The corresponding kinetic parameters (activation energy of thermal decomposition) were computed by nonlinear regression which was the iterative calculation of the minimum sum of least squares.

Synthesis of triblock copolymers

A typical experimental procedure was presented as Scheme 1 to synthesize linear triblock copolymer. A solution mixture of initiator of polymerization (AIBN, 0.04 g, 0.25 mmol), and RAFT chain transfer agent (CDB, 0.13 g, 0.5 mmol), and monomer of first block (*t*BMA, 8.17 g, 57.60 mmol) in a solvent of benzene (10.0 mL) was degassed by a process of three freeze-pump-thaw cycles. The above mixture was then thermostated by oil bath at 60 °C under an argon atmosphere. After 10 h, a monomer of the second block (GMA, 5.35 g, 37.60 mmol) was added to the polymerization reaction system, after 2 h the reaction system was quenched into liquid nitrogen. The reaction mixture was diluted with THF and then precipitated into a suitable mixture of methanol–water (1:1, v/v, total volume 800 mL). The product was dried under vacuum to constant weight with $M_{n,GPC} = 1.23 \times 10^4$ g mol^{-1}, $M_w/M_n = 1.21$.

The resulting diblock copolymer (P*t*BMA-*b*-PGMA-SSZ) was used as a polymeric chain transfer agent to initiate polymerization of styrene, to get the third block of copolymer. Thus, a solution of styrene (12.7 g, 0.12 mol), macro-CTA (4.90 g, 0.40 mmol), and AIBN (0.03 g, 0.2 mmol) in a solvent of benzene (12 mL) was degassed once again. The mixture was then thermostated at 60 °C under an argon atmosphere and stopped by being quenched into liquid nitrogen at a predetermined time. The reaction mixture was diluted with THF (6 mL) and precipitated into a mixture of methanol–water (1:1, v/v, total volume 800 mL). The

Scheme 1 Representative synthesis route of triblock copolymer
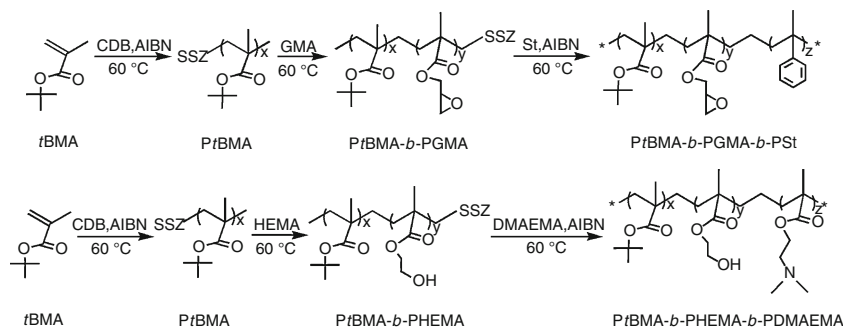
polymer was dried under vacuum to a constant weight with $M_{n,GPC} = 2.23 \times 10^4$ g mol^{-1}, $M_w/M_n = 1.25$. A different linear triblock copolymer of PtBMA-b-PHEMA-b-PDMA-EMA was synthesized with a different mole dosage of reagent by the same RAFT polymerization procedure as the above and is represented as shown Scheme 1. The medium AB diblock copolymer PtBMA-b-PHEMA and the final linear triblock copolymer PtBMA-b-PHEMA-b-PDMA-EMA had their number-average molecular weight of 1.95×10^4 and 4.4×10^4 g mol^{-1} with their corresponding polydispersity indexes 1.25 and 1.35, respectively, as shown in Fig. 1.

Results and discussion

Characterization of linear triblock copolymers

GPC chromatographs (Fig. 1) show that the triblock copolymers, which were prepared by controlled/living radical polymerization mediated by the RAFT process, have an incremental growth of molecular weight because the number-average molecular weight increased with the lapse of polymerization time and finally the number degree of polymerization of the polymer segment increased during the whole RAFT polymerization process as a result, indicating a living feature of polymerization. The molecular weight $M_{n,GPC}$ of final triblock copolymer PtBMA-b-PGMA-b-PSt was 2.23×10^4 g mol^{-1} (Fig. 1a) and with a narrow distribution of polydispersity index M_w/M_n of 1.25, while the triblock copolymer PtBMA-b-PHEMA-b-

PDMAEMA has a $M_{n,GPC}$ of 4.4×10^4 g mol^{-1} (Fig. 1b) and M_w/M_n of 1.35 as shown in Table 1.

FT-IR spectra of two different triblock copolymers, PtBMA-b-PGMA-b-PSt (Fig. 2a) and PtBMA-b-PHEMA-b-PDMAEMA (Fig. 2b), show that the most obvious spectral features of them are C–H of alkyl from PtBMA segment at 3,100–2,800 cm^{-1}, ubiquitous C=O carbonyl stretching at 1,720 cm^{-1}, and the vibration of t-butyl groups at 1,360 and 1,380 cm^{-1}. The peak at 3,400 cm^{-1} is indicative of the active hydroxyl group of PtBMA-b-PHEMA-b-PDMAEMA (Fig. 2b), while the same peak is an irrelevancy of impurity (water) due to the interference from moisture in the FT-IR spectra of PtBMA-b-PGMA-b-PSt (Fig. 2a). The skeletal vibrations of epoxy ring at 830 cm^{-1} are a witness for the middle segment PGMA and the phenyl group at 710 cm^{-1} as an another evident signal for the segment of PSt (Fig. 2a). While the peaks at 2,800–2,700 cm^{-1} are a characteristic presence of CH$_3$-N groups for the segment PDMAEMA (Fig. 2b).

^{1}H-NMR spectra of triblock copolymer (Fig. 3) show that the signals of aromatic, epoxy, and t-butyl protons are observed obviously at 6.3–7.5, 2.5–4.4, and 1.4 ppm, respectively, in the spectra of PtBMA-b-PGMA-b-PSt (Fig. 3A, B). The signals of t-butyl and $-CH_2^*N(CH_3)_2$ protons were distinctly observed at 1.4 and 2.2–2.6 ppm, respectively, in the spectra of PtBMA-b-PHEMA-b-PDMA-EMA (Fig. 3C, D). However, the proton signals of the $-CH_2^*CH_2^*-$ groups were slightly observed at 3.6–4.2 ppm for PtBMA-b-PHEMA-b-PDMAEMA.

From these data above when the integral intensity of aromatic signal at 7.9 ppm in the ^{1}H-NMR was set as one

Fig. 1 GPC chromatographs of triblock copolymer: PtBMA-b-PGMA-b-PSt (**a**) and PtBMA-b-PHEMA-b-PDMAEMA (**b**)
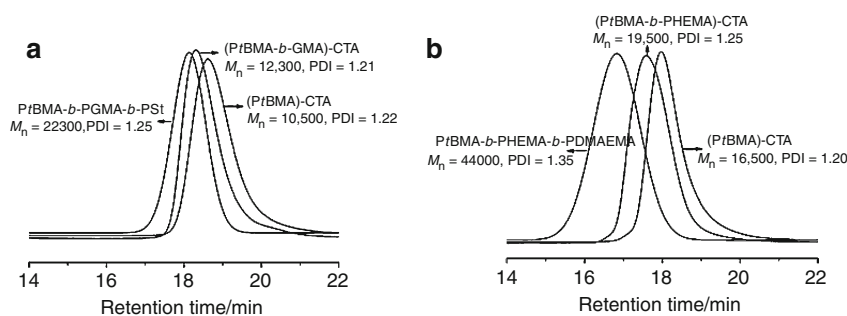
Table 1 Copolymer synthesized by RAFT polymerization technique

Block copolymer	Degree of polymerization (DP)	$M_{n,NMR}$	PDI
PtBMA-b-PGMA	PtBMA$_{97}$-b-PGMA$_{18}$	16,602	1.21
PtBMA-b-PHEMA	PtBMA$_{137}$-b-PHEMA$_{23}$	22,716	1.25
PtBMA-b-PGMA-b-PSt	PtBMA$_{97}$-b-PGMA$_{18}$-b-PSt$_{98}$	28,166	1.25
PtBMA-b-PHEMA-b-PDMAEMA	PtBMA$_{137}$-b-PHEMA$_{23}$-b-PDMAEMA$_{156}$	47,208	1.35
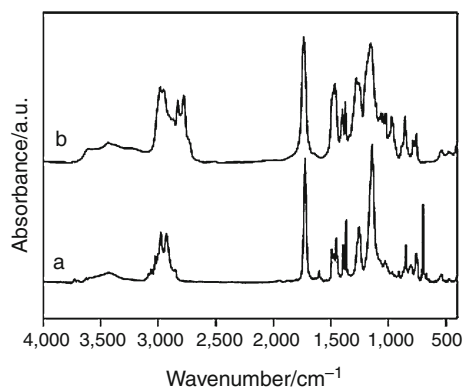
Fig. 2 FT-IR spectra of triblock polymer: PtBMA-b-PGMA-b-PSt (*a*) and PtBMA-b-PHEMA-b-PDMAEMA (*b*)

unit that the number degree of polymerization of different segments in the triblock copolymer PtBMA-b-PGMA-b-PSt and PtBMA-b-PHEMA-b-PDMAEMA can be evaluated and structure can be determined as well (Table 1).

The ^{1}H-NMR spectra of the sequential polymerization products are shown in Fig. 3, in which A (C) and B (D) correspond to the intermediate diblock PtBMA-b-PGMA (PtBMA-b-PHEMA) and the final triblock copolymer PtBMA-b-PGMA-b-PSt (PtBMA-b-PHEMA-b-PDMAEMA), respectively. In the former, signals of aromatic protons of the end group (derived from the RAFT agent) are visible between 7.4 and 7.9 ppm. From integrations of the aromatic signal at 7.9 ppm (peak i in Fig. 3A) and those of t-butyl (1.4 ppm, peak a in Fig. 3A and B), epoxy groups (2.5–4.4 ppm, peak b, c, and d in Fig. 3A and B) and protons in the benzene ring of PSt (6.7–7.2 ppm, peak e in Fig. 3B). While the ratio of integral peak area between different protons in distinct polymer segments shows that $2H_i:2H_d = 1:18.0$, $2H_i:9H_a = 1:436.5$, and $2H_i:5H_e = 1:245.0$, respectively.

By using the following calculated formula: $2H_i/nH = 1/(\text{integral peak area/DP})$, then DP $= 2 \times$ integral peak area/n, the value of 2 represent two protons in the peak i of ^{1}H-NMR spectra (Fig. 3A, C) and the integral area for two protons of H_i was set as one unit 1, while n is the number of protons in each calculated monomeric unit, and then the degrees of polymerization of GMA and tBMA in diblock
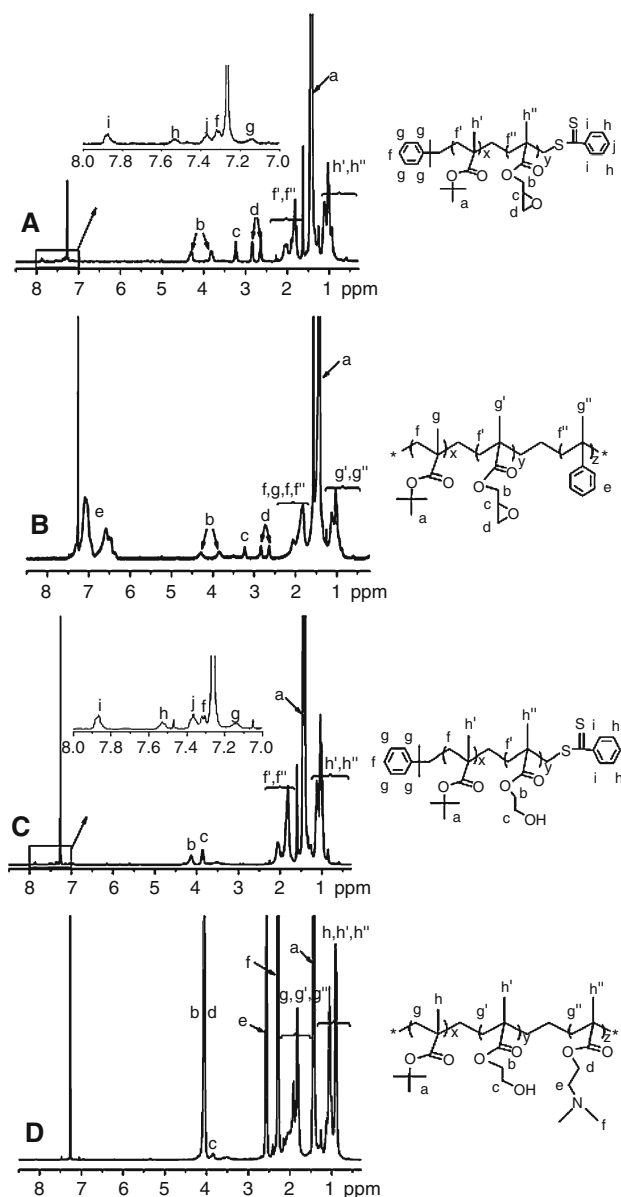
Fig. 3 ^{1}H-NMR spectra of PtBMA-b-PGMA-CTA (**A**), PtBMA-b-PGMA-b-PSt (**B**), PtBMA-b-PHEMA-CTA (**C**), and PtBMA-b-HEMA-b-PDMAEMA (**D**)

PtBMA-b-PGMA are calculated to be DP$_{GMA} = 18.0 \times 2/2 = 18$ and DP$_{tBMA} = 436.5 \times 2/9 = 97$, respectively. As a result, the degree of polymerization of styrene (DP$_{St}$) is $245.0 \times 2/5 = 98$ as determined from the spectrum of the triblock copolymer PtBMA-b-PGMA-b-PSt as well (Fig. 3B), resulting in an estimation of $M_{n,NMR} = 2.81 \times 10^4$ g mol^{-1}. By the same way, the degrees of polymerization of tBMA, HEMA and DMAEMA in triblock copolymer PtBMA-b-PHEMA-b-PDMAEMA were determined to be 137, 23, and 156 according to the $2H_i:9H_a = 1:616.0$, $2H_i:4H_{b+c} = 1:46.0$ (Fig. 3C), and $2H_i:3H_f = 1:234.0$ (Fig. 3D), respectively, with $M_{n,NMR} = 4.72 \times 10^4$ g mol^{-1} as a consequence.

The number degrees of polymerization (DP) and the number-average molecular weight ($M_{n,NMR}$) of three segments in the two linear triblock copolymers were, therefore, quantificationally evaluated by the ^{1}H-NMR, while polydispersity index (PDI) was evaluated from the GPC chromatographs (Table 1).

Thermal properties and kinetics analysis

The TG profile of thermal decomposition progresses for two different ABC linear triblock copolymers and their medium products (homopolymer and AB block copolymers) in the synthesis process are shown in Fig. 4, and the more detailed and exact thermal decomposition progresses of the two linear triblock copolymers, DTG curves (DTG-d, DTG-e), are shown in Fig. 5 as well. The homopolymer PtBMA (Fig. 4a) was taken from the synthesis process of the PTHD.

From Fig. 4 we can clearly observe that it puts up three main thermal loss steps both in these polymers; meanwhile, an interesting phenomenon takes place that the thermal stability increased as the addition of different segments into the final triblock copolymer because the thermal decomposition temperature of them had shifted to the higher site according to the same decomposition ratio. The AB copolymer of PtBMA-b-PGMA (Fig. 4c) was presumedly took the intermolecular crosslinking reaction due to the oxirane rings of second segment PGMA are typically reactive, and with the inducement of suitable heat, which result in the thermal stability was higher than that of the homopolymer PtBMA (Fig. 4a) during the thermal decomposition. While, the thermal stability of AB diblock copolymer PtBMA-b-PHEMA (Fig. 4b) was higher than that of PtBMA which may due to the loss of the water from the hydroxyl groups of the second segment PHEMA in the PtBMA-b-PHEMA, the resulting medium product of the

intermolecular reaction dominated the higher thermal property contrasting with the homopolymer of PtBMA during the thermal decomposition.

A summary of the TG results for the two linear triblock copolymers under dynamic nitrogen atmosphere is shown as Table 2. It could be seen that the main TG profile of triblock copolymers is similar to each other under nitrogen atmosphere that the two copolymers both have two obvious decomposition phases (Fig. 5). However, we can observe that the TG profile of PTGS (TG-e) was shifted to the higher thermal temperature contrasting with PTHD (TG-d) at the same mass loss. This could also be explained—the higher the onset in the thermal progresses, the higher the stability of the copolymer is. Actually, the extrapolated onset temperature of PTGS is 235.7 °C which is higher than that of the PTHD (222.5 °C). However, the principal ingredient in the homopolymer of PtBMA (Fig. 4a), diblock copolymer of PtBMA-b-PGMA (Fig. 4b) and PtBMA-b-PHEMA (Fig. 4c) of tBMA, according to their weight ratios are 100, 83.0, and 85.6 wt%, respectively. So their thermal stabilities of these polymers did not display distinct difference even when the second segment was introduced into the diblock copolymers. Nevertheless, things change for the triblock copolymers because the heat resistance of benzene ring of third segment PSt from PTGS is much higher than that from the segment PDMAEMA introduced into the PTHD.

The TG curves corresponding to the copolymers exhibit some common characteristics during the thermal decomposition, and the data are shown in Table 2.

The TG analyses of the sample were adopted after 100 °C, in respect that a nonsignificant mass loss before 100 °C due to the humidity from the air or the reaction reagent from the chemosynthesis procedure of the copolymers which is unimportant for our further discussion.
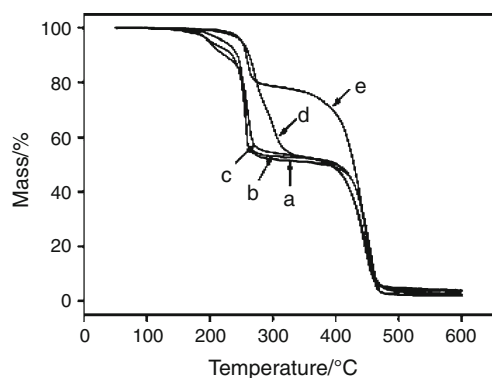
Fig. 4 TG curves obtained for a heating rate of 20 °C min^{-1} under dynamic nitrogen atmosphere: homopolymer PtBMA (a), AB block copolymer PtBMA-b-PGMA (b), PtBMA-b-PHEMA (c), ABC triblock copolymer PtBMA-b-PHEMA-b-PDMAEMA (PTHD) (d), and PtBMA-b-PGMA-b-PSt (PTGS) (e)
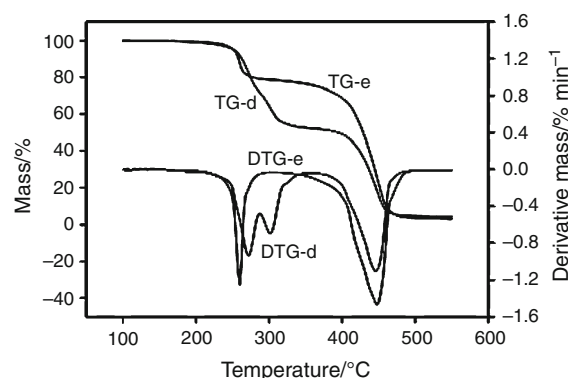
Fig. 5 TG and DTG curves obtained for a heating rate of 20 °C min^{-1} under dynamic nitrogen atmosphere: PtBMA-b-PHEMA-b-PDMAEMA (PTHD) (d) and PtBMA-b-PGMA-b-PSt (PTGS) (e)

The first mass loss step corresponds to the loss of *t*-butyl groups and part poly(*t*-butyl methacrylate) (P*t*BMA) carbon chains from the first segment of triblock copolymers (Fig. 5). It presumably includes some water from hydroxyl group of the middle segment PHEMA in the PTHD during this mass loss step as well (Fig. 5d).

The second mass loss corresponds to the loss of remnant P*t*BMA and the other two segments of the triblock copolymer of PTGS (Fig. 5e), this course mostly due to the thermal stability of intermediate product from the intermolecular crosslinking reaction of the oxirane ring from the segment PGMA and the rigid aromatic ring from the third segment of PSt, which the DTG curves can be observed only a bigger second thermal decomposition rate peak at 447.5 °C. While for PTHD (Fig. 5d), the second mass loss corresponds to remnant P*t*BMA, and part of middle segment PHEMA. The content of the former two segments of P*t*BMA and PDHEMA in PTHD was 47.5% (Table 3), and this theoretical value agreed well with the former two mass losses (47.4% in Table 2) in the triblock copolymer as well. These data illustrated that the decompositions of segment P*t*BMA and PDHEMA in PTHD took place in the primary and secondary mass loss steps, in which the primary mass loss was due to the decomposition of *t*-butyl groups, a majority of P*t*BMA and minor part of PHEMA, and then it can be deduced that the secondary mass loss (19.2%) was due to the decomposition of remnant P*t*BMA and PHEMA.

Table 2 TG results for triblock copolymer P*t*BMA-*b*-PGMA-*b*-PSt (PTGS) and P*t*BMA-*b*-PHEMA-*b*-PDMAEMA (PTHD) under nitrogen atmosphere when $\beta = 20$ °C min^{-1}

Entry	PTGS	PTHD
Onset temperature T/°C	235.7	222.5
Primary region T/°C	170–312.5	142.5–287.5
Primary mass loss/%	21.5	28.2
Secondary region T/°C	312.5–505	287.5–355
Secondary mass loss/%	74.7	19.2
Tertiary region T/°C	–	355–530
Tertiary mass loss/%	–	48.0
Residue at 550 °C/%	3.52	4.47

Table 3 Segment contents of triblock copolymer P*t*BMA-*b*-PGMA-*b*-PSt (PTGS) and P*t*BMA-*b*-PHEMA-*b*-PDMAEMA (PTHD) calculated from the results of ^{1}H-NMR

Entry	PTGS	PTHD
First segment/%	48.9	41.2
Second segment/%	9.1	6.3
Third segment/%	41.0	51.9
CDB/%	1.0	0.6

DTG curves (Fig. 5d) show that an additional third mass loss is observed for the copolymer PTHD which due to the decomposition from the remnant segment PHEMA and segment PDMAEMA. The element of nitrogen (N–(CH$_3$)$_2$) in the PDMAEMA stand a good chance for that this segment take mass loss in this step.

The kinetic decomposition of the copolymers was analyzed with the following two nonisothermal thermokinetic analysis techniques to study the thermal decomposition of the two linear triblock copolymers. The process of thermokinetic analysis should be run above 100 °C to insure total vaporization of water from the atmosphere or reactants.

Friedman differential method

Friedman developed a differential isoconversional method whereby the activation energy for a mass loss process could be determined from the Eq. 3 [12–14]:

$$\ln\left(\frac{\beta d\alpha}{dT}\right) = \ln[Af(\alpha)] - \frac{E}{RT} \tag{1}$$

and

$$\frac{d\alpha}{dt} = \frac{\beta d\alpha}{dT}. \tag{2}$$

Then

$$\ln\left(\frac{d\alpha}{dt}\right) = \ln[Af(\alpha)] - \frac{E}{RT} \tag{3}$$

where β is the heating rate, T is the temperature, t is the time, R is the gas constant, α is the conversion degree, A is the pre-exponential factor, and E is the activation energy in sense of Arrhenius equation. The slope of the straight line obtained by plotting $\ln(d\alpha/dt)$ vs. $1/T$ at any level of same conversion degree (α) can be used to calculate the activation energy for the mass loss process of the copolymers under nitrogen atmosphere. A typical calculated plot for copolymers under nitrogen atmosphere by this differential method is shown in Figs. 6 and 7.
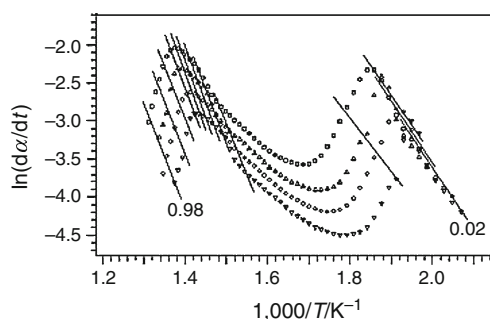
Fig. 6 Friedman analysis of P*t*BMA-*b*-PGMA-*b*-PSt (PTGS)
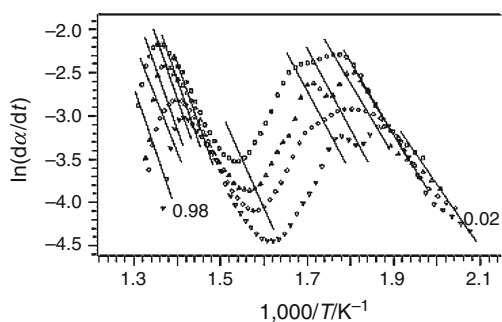
Fig. 7 Friedman analysis of P*t*BMA-*b*-PHEMA-*b*-PDMAEMA (PTHD)

Ozawa–Flynn–Wall integral method

Ozawa (1965), Flynn–Wall (1966), and Doyle (1962) developed a well-known integral isoconversional method which can determine the activation energy for a mass loss process of the two triblock copolymers as well by using Eq. 11 as follows [15, 16, 18]:

First, two basic equations at the beginning of kinetic analysis can be set asdifferential formula:

$$f(\alpha) = A \exp\left(-\frac{E}{RT}\right)\frac{d\alpha}{dt} \qquad (4)$$

and integral formula:

$$G(\alpha) = A \exp\left(-\frac{E}{RT}\right)t \qquad (5)$$

while they have a relationship of:

$$f(\alpha) = \frac{1}{G'(\alpha)} = \frac{1}{d[G(\alpha)]/d\alpha} \qquad (6)$$

therefore, the Eq. 6 can be changed as:

$$\int_0^\alpha d[G(\alpha)] = \int_0^\alpha \frac{d\alpha}{f(\alpha)} \qquad (7)$$

then,

$$G(\alpha) = \int_0^\alpha \frac{d\alpha}{f(\alpha)} = \frac{A}{\beta}\int_{T_0}^T \exp\left(\frac{-E}{RT}\right)dT \qquad (8)$$

with

$$\beta = \frac{dT}{dt} \qquad (9)$$

Then Eq. 8 is changed as:

$$\ln G(\alpha) = \ln\left(\frac{AE}{R}\right) - \ln\beta - 5.3305 + 1.052\frac{E1}{RT}, \qquad (10)$$

finally

$$\ln\beta = \ln\left(\frac{AE}{R}\right) - \ln G(\alpha) - 5.3305 + 1.052\frac{E1}{RT} \qquad (11)$$

where β is the heating rate, T is the temperature, R is the gas constant, α is the degree of conversion, $G(\alpha)$ is a integral format for the function of $1/f(\alpha)$ between 0 and α, A is the pre-exponential factor, and E is the Arrhenius activation energy. The plot of $\ln\beta$ vs. $1/T$ can give the slope $1.052~E/R$ by which the activation energy at any given same conversion degree for the mass loss process of copolymers. This isoconversional integral method that can calculate the activation energy E at a particular α for the two triblock copolymers under nitrogen atmosphere is shown in Fig. 8.

The activation energy (E) of the copolymer samples are evaluated by the Friedman (Fig. 9a, b) and OFW (Fig. 9c) analyses during the thermal degradation at 5, 10, 20, and 40 °C min^{-1} under nitrogen atmosphere is shown as Fig. 9. As can be seen from the thermal decomposition of PTGS (Fig. 9a), the activation of it is more than that of PTGS on the whole. While it is subtle that the activation energy is
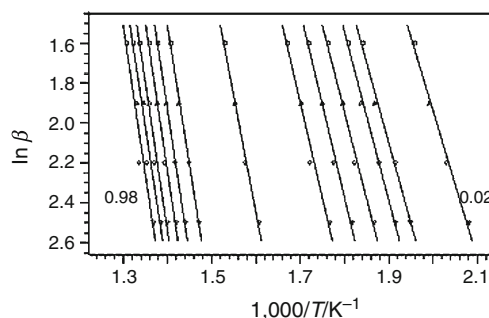
Fig. 8 Ozawa–Flynn–Wall analysis of P*t*BMA-*b*-PHEMA-*b*-PDMA-EMA (PTHD)
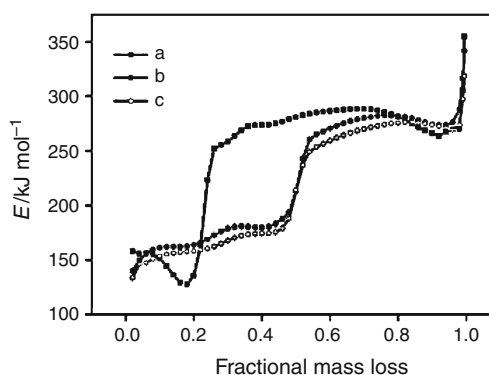
Fig. 9 Activation energy plotted from isoconversional thermokinetic analysis: Friedman analysis result for P*t*BMA-*b*-PGMA-*b*-PSt (PTGS) (*a*), Friedman analysis result for P*t*BMA-*b*-PHEMA-*b*-PDMAEMA (PTHD) (*b*), and OFW analysis result for P*t*BMA-*b*-PHEMA-*b*-PDMAEMA (PTHD) (*c*)

the lowest according to the conversion degree (α) was 0.19 in the two linear triblock copolymers that agrees well with the DTG-e curve at the $\alpha = 0.188$ which exhibits a sharp shape of energy, this energy vale due to a larger thermal decomposition rate (Fig. 5e) contrasting with PTHD. A slight turning point occurs at $\alpha = 0.25$ that means the first mass loss step stops at here and the second mass loss begins at the same time. After that the activation energy of PTGS was markedly higher than that of copolymer PTHD (Fig. 9b) before α at 0.8 because the heating resistance of PTGS preponderates remarkably over that of the triblock copolymer PTHD. Consequently, a less sharp energy peak presents at α of 0.92 in the second mass loss step after 463 °C, due to the burnout of the residual carbonaceous material from the previous steps.

Although, its similar behavior to the other one occurs after $\alpha = 0.94$ because of the combustion of carbonaceous residue, copolymer PTHD presents a quite different behavior from the PTGS during the whole thermal decomposition process (Fig. 9b) which was composed of three mass loss steps. It is another distinct phenomenon where it can be observed that the thermal stability of PTHD was not as good as PTGS. It can be taken as a complementary witness that the intermediate product from oxirane rings that had took the intermolecular reaction during the thermal decomposition and rigid aromatic rings sited in the block segments of the latter copolymer shows an excellent heating resistance which can be confirmed by the results of TG curve. At the same time, the mass loss range of DTG curve (Fig. 5d) fits well with the first two energy vales in the activation energy plot (Fig. 9b). To validate the result of Friedman's analysis, an activation energy plotted from isoconversional integral method, OFW analysis, was calculated for the PTHD in the Fig. 9c as well. It is homologous at a certain extent that these two isoconversional analyses had both illustrated the same tendency chart in activation energy even if the activation energy from Friedman analysis is a little more than that from OFW analysis.

Conclusions

Two different linear triblock copolymers P*t*BMA-*b*-PGMA-*b*-PSt and P*t*BMA-*b*-PHEMA-*b*-PDMAEMA based on methacrylate ester were synthesized with RAFT polymerization technique.

Physical characterization of GPC shows that chemosynthesis process of these copolymers has a ubiquitous character of controlled radical polymerization especially in the number-average molecular weight and number-average degree of polymerization. FT-IR and ^{1}H-NMR spectra further show that the characteristic groups correspond well to the preconcerted molecular structure of the triblock copolymers.

The result of nonisothermal kinetic analysis fits well with the thermogravimetry analysis during the thermal decomposition of polymer segment. Isoconversional thermokinetic analysis of Friedman differential method and OFW integral method complementarily indicates that the thermal stability of P*t*BMA-*b*-PGMA-*b*-PSt is much higher than that of P*t*BMA-*b*-PHEMA-*b*-PDMAEMA, which due to the intermolecular crosslinking reaction had taken place among the oxirane rings in the segment PGMA of linear triblock copolymer P*t*BMA-*b*-PGMA-*b*-PSt, which are typically reactive under the suitable heat, and aromatic groups are introduced into the copolymer of the former.

References

1. Shen J, Hu Y, Li C, Qin C, Ye M. Synthesis of amphiphilic graphene nanoplatelets. Small. 2009;5:82–5.
2. Cheng J, He J, Li C, Yang Y. Facile approach to functionalize nanodiamond particles with v-shaped polymer brushes. Chem Mater. 2008;20:4224–30.
3. Mayya KS, Schoeler B, Caruso F. Preparation and organization of nanoscale polyelectrolyte-coated gold nanoparticles. Adv Funct Mater. 2003;13:183–8.
4. Zhang M, Liu L, Zhao H, Yang Y, Fu G, He B. Double-responsive polymer brushes on the surface of colloid particles. J Colloid Interface Sci. 2006;301:85–91.
5. Li D, He Q, Cui Y, Li J. Fabrication of pH-responsive nano-composites of gold nanoparticles/poly(4-vinylpyridine). Chem Mater. 2007;19:412–7.
6. Wang D, Duan H, Möhwald H. The water/oil interface: the emerging horizon for self-assembly of nanoparticles. Soft Matter. 2005;1:412–6.
7. Binder WH. Supramolecular assembly of nanoparticles at liquid–liquid interfaces. Angew Chem Int Ed. 2005;44:5172–5.
8. Li D, Sheng X, Zhao B. Environmentally responsive "hairy" nanoparticles: mixed homopolymer brushes on silica nanoparticles synthesized by living radical polymerization techniques. J Am Chem Soc. 2005;127:6248–56.
9. Lin Y, Skaff H, Böker A, Dinsmore AD, Emrick T, Russell TP. Ultrathin cross-linked nanoparticle membranes. J Am Chem Soc. 2003;125:12690–1.
10. Skaff H, Lin Y, Tangirala R, Breitenkamp K, Böker A, Russell TP, Emrick T. Crosslinked capsules of quantum dots by interfacial assembly and ligand crosslinking. Adv Mater. 2005;17:2082–6.
11. Chrissafis K. Kinetics of thermal degradation of polymers. J Therm Anal Calorim. 2009;95:273–83.
12. Lin B, Yang L, Dai H, Hou Q, Zhang L. Thermal analysis of soybean oil based polyols. J Therm Anal Calorim. 2009;95:977–83.
13. Friedman HL. Kinetics of thermal degradation of char-foaming plastics from thermogravimetry: application to a phenolic resin. J Polym Sci. 1965;6C:183–95.
14. Vlase T, Vlase G, Doca N. Kinetics of thermal decomposition of alkaline phosphates. J Therm Anal Calorim. 2005;80:207–10.

15. Pratap A, Lilly Shanker Rao T, Lad K, Dhurandhar HD. Iso-conversional vs. model fitting methods. J Therm Anal Calorim. 2007;89:399–405.
16. Vyazovkin S. Model-free kinetics. J Therm Anal Calorim. 2006; 83:45–51.
17. Le TPT, Moad G, Rizzardo E, Thang SH. PCT International Patent Application (Int Pat Appl) WO 9801478 A1 980115, 1998.
18. Starink MJ. On the applicability of isoconversion methods for obtaining the activation energy of reactions within a temperature-dependent equilibrium state. J Mater Sci. 1997;32:6505–12.